Thermal performance assessment and improvement of a solar domestic hot water tank with PCM in the mantle

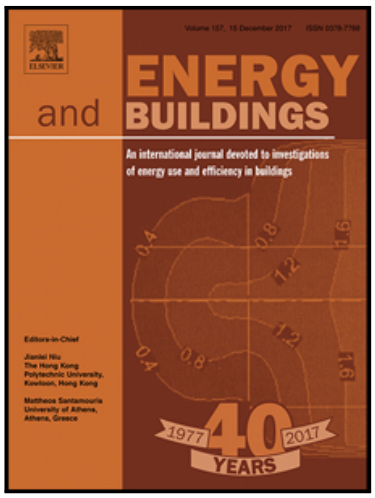

Thermal performance assessment and improvement of a solar domestic hot water tank with PCM in the mantle

Jie Deng , Simon Furbo , Weiqiang Kong , Jianhua Fan

PII: S0378-7788(17)32695-6
DOI: 10.1016/j.enbuild.2018.04.058
Reference: ENB 8531

To appear in: *Energy & Buildings*

Received date: 6 August 2017
Revised date: 9 March 2018
Accepted date: 23 April 2018

Please cite this article as: Jie Deng , Simon Furbo , Weiqiang Kong , Jianhua Fan , Thermal performance assessment and improvement of a solar domestic hot water tank with PCM in the mantle, *Energy & Buildings* (2018), doi: 10.1016/j.enbuild.2018.04.058

Highlights:

- Heat transfer matching properties of a prototype solar DHW tank were analyzed via tests.
- Thermal performance of the improved tank was ameliorated except the bottom spiral.
- Heat content of PCM is somewhat lower than that of ideally working SAT.
- The PCM tends to be stable without performance degradation via 3-months tests.

*Manuscript for **Energy and Buildings***

Thermal performance assessment and improvement of a solar domestic hot water tank with PCM in the mantle

Jie Deng [a,b,c,*], Simon Furbo [b], Weiqiang Kong [b], Jianhua Fan [b]

[a] School of Engineering and Physical Sciences, Heriot-Watt University, Edinburgh, Scotland, EH14 4AS, UK

[b] Department of Civil Engineering, Technical University of Denmark, Brovej 118, Kgs. Lyngby, DK 2800, Denmark

[c] Institute of Electrical Engineering, Chinese Academy of Sciences, Beijing 100190, P R China

* Corresponding author:

School of Engineering and Physical Sciences, Heriot-Watt University, Edinburgh, Scotland, EH14 4AS, UK

E-mail address: deng-jie2@163.com; j.deng@reading.ac.uk (J. Deng)

Thermal performance assessment and improvement of a solar domestic hot water tank with PCM in the mantle

Abstract

To develop an appropriate solar DHW (Domestic Hot Water) tank for residential dwellings and put it into the European solar thermal market for promotion, thermal performance tests of PCM (Phase Change Material) hot water storage tanks of both a prototype and an improved version with a water volume of 148 l and 35 kg PCM in the mantle has been carried out. The tank was designed to provide DHW for residential dwellings through a combination of solar and auxiliary heating, concurrently using PCM on the basis of cheap SAT (Sodium Acetate Trihydrate) as a thermal battery to shave off peak auxiliary power or to work under power outage. Heat transfer matching properties of the bottom and the top spirals separately for solar charge and auxiliary charge of the prototype DHW tank were ascertained in terms of heat exchanger capacity rate (HXCR) and the rule of thumb of boiler powers, respectively. Moreover, heat content of the PCM was estimated via a series of test cycles in order to infer its capacity and stability. It was found that there were some technical problems for the prototype tank module, such as mismatching property of the heat exchanger spirals, heat mixing phenomena during hot water draw-off. Thus, an improved tank was manufactured based on the test results of the prototype. Further tests indicated that the matching property of the top heat exchanger spiral was ameliorated for auxiliary charge and the heat mixing between hot water supply pipe

and water tank was restrained during discharge, except that the length of the bottom spiral should be further reduced. Regarding the PCM in the mantle, it was inferred that the PCM heat content was somewhat lower than that of ideally working SAT. The PCM tended to perform stably under 16 test cycles with more than 3-month consecutive tests, implying no phase segregation occurred as that would degraded its performance.

Keywords: Solar DHW tank; Heat exchanger spirals; Thermal performance; Heat exchange capacity rate (HXCR); PCM heat storage

1 Introduction

Making full use of solar thermal energy for Domestic Hot Water (DHW) supply is one of the effective ways of saving energy in residential buildings. Today in Europe, marketed solar tanks for small solar DHW systems are either based on inexpensive standard hot water tanks or relatively expensive specially designed tanks suitable for solar DHW systems [1, 2]. Consequently, there is a need to develop solar tanks based on cheap standard tanks suitable for solar DHW systems for mass production.

In terms of conventional DHW storage tanks regardless of solar thermal, plenty of efforts had been made by researchers or engineers to improve the energy efficiency of the tanks, encompassing heat charging and discharging characteristics of DHW tanks, tank thermal stratification, tank heat loss, PCM heat storage, etc. Fernández-Seara et al. [3] analyzed the dynamic mode of operation of a domestic electric hot water storage tank with a capacity of 150 l through experiment taking into account six possible-inlet-outlet port arrangements and water draw-off flow rates of 5, 10 and 15 l/min. The inlet-outlet port configuration (i2-o1 in their study) was identified as the best one and was proposed to use in practice. Abdelhak et al. [4] undertook three-dimensional CFD analysis on the flow characteristics and thermal stratification evolution of a DHW storage tank during charging and discharging phases. They revealed that the vertical orientation design was more efficient than the horizontal one for a stratified storage tank. González-Altozano et al. [5] developed a new method called Virtual TC for the thermal performance characterisation in a hot water storage

tank during charge, allowing estimation of water temperature at any depth and time during charge. In the aspect of tank thermal stratification during DHW discharge, Castell et al. [6] studied the suitability of the most used dimensionless numbers for characterizing stratification in water tanks and found that Richardson number was the best number to define stratification in a water tank, while Mix number presented some problems and a bad behavior. As to the inlet effect, Moncho-Esteve et al. [7] analyzed the influence of simple inlet devices on the thermal stratification of a cylindrical hot water storage tank by CFD techniques and reported that a sintered bronze conical diffuser could improve stratification compared to a conventional bronze elbow inlet. As a matter of fact, there is lots of similar work in relation to various types of inlet stratifiers or devices for the sake of establishing tank thermal stratification during charge, with a view to reducing the mixing process and improving energy efficiency. Andersen et al. [8] investigated four inlet stratification pipes, two rigid pipes with openings and two double-layer fabric pipes to show advantages and disadvantages of the pipes under applied operation conditions. Dragsted et al. [9] conducted experimental work on a small, high and slim polymer tank design with differently designed inlet stratifiers under different controlled laboratory conditions and elucidated the suitability of differently designed inlet stratifiers during the tests. Their tests showed that both types of inlet stratifiers had an ability to create stratification. Some other inlet stratifier devices, such as a novel equalizer proposed by Wang et al. [10], a new helical flow distributor designed by Zachár [11], also work well according to their reports. Besides, tank heat loss characteristic is also worthy of concern. Fan

and Furbo [12, 13] elucidated the mechanisms of thermal stratification in a hot water tank established by heat loss from the tank and the buoyancy driven flow in a hot water tank due to standby heat loss. Cruickshank and Harrison [14] reported the heat loss characteristics of a solar DHW tank which was essentially a commonplace tank as it adopted an external heat exchanger loop to store solar heat.

With regard to PCM heat storage tanks, Cabeza et al. [15] chose a granular PCM–graphite compound of about 90 vol. % of sodium acetate as a PCM and tested the thermal performance of a hot water storage tank with different numbers of PCM cylinder modules at the top of tank. Nabavitabatabayi et al. [16] numerically investigated the impact of integration of nano-particle PCMs on the thermal performance of a hot water tank and demonstrated that the integration of the enhanced PCMs to the hot water tank could shift the power demand to the off-peak for a longer period of time compared to pure PCMs due to the higher thermal conductivity and the enhanced heat transfer rate. The work by Nkwetta et al. [17] and Najafian et al. [18] disclosed a similar viewpoint as in [16] that the combination of PCMs with DHW tanks could enable to shift electrical energy consumption to off peak periods and consume less energy compared to the regular ones without PCMs, considering SAT (90%) and graphite (10%) composite as the PCM.

The aforementioned work was mainly concerned on hot water tanks excluding solar thermal application. Aiming to solar DHW storage tanks, matching property of the

tanks with solar collectors or solar thermal systems is of significance considering a good degree of thermal stratification. During the last 30 years, researchers, engineers and manufacturers had been pursuing an attractive low fluid flow rate solar DHW system, employing a flow rate range of 0.15 to 0.25 l/min per m^2 collector in the solar loops [1, 2]. The reason can be traced back to the investigations carried out in the 1970s and 1980s in the Netherlands and Denmark, which disclosed that the thermal performance of low flow solar DHW systems is 10–25% higher than that of traditional solar heating systems and that the amount of limescale deposits in the hot water tanks is lower for low flow systems than for traditional systems, resulting in increased durability [19]. Furthermore, the performance-to-cost ratio of low flow solar heating systems can be improved by about 20–40% due to a cheaper system cost [20]. To develop such a cost-effective solar tank, plenty of design ways have been introduced by researchers and engineers, since the solar heat can be transferred to a solar tank by means of a built-in heat exchanger spiral with a long vertical height, a mantle welded around the lower part of a hot water tank or an external heat exchanger and more or less advanced designs of the heat transfer loop used to transfer solar heat from the heat exchanger to the solar tank [1, 2]. Especially, the mantle tank for low flow solar DHW systems is highly concerned amongst different ways of tank designs, as thermal stratification can be easily established in the tank during charge with a low flow rate in the mantle [21, 22], resulting in a high thermal performance of the solar DHW systems. Dehghan and Barzegar [23] numerically investigated the transient thermal behavior of a vertical storage tank applied in a domestic solar water heating

system with a mantle heat exchanger in the discharge mode. They found that the tank inflow Reynolds number and/or its inflow port diameter should be kept below certain values in order to have a tank with a proper thermal performance and/or have least mixing inside the tank during the consumption period. Besides, Arslan and Igci [24] presented the influence of the operating parameters during discharging / consumption mode on the thermal performance of a vertical solar storage tank with a mantle heat exchanger installed in a solar DHW system.

In addition to the design way of solar tanks, the design of the cold water inlet for hot water tanks also plays a pivotal role for establishing good thermal stratification. This is similar to the effect of inlet stratifiers for conventional DHW tanks mentioned previously. It is verified that by making use of a cold water inlet with a suitable baffle plate, the thermal performance of marketed Danish solar DHW systems can be improved by about 5% [25, 26]. There are also some work involving PCM heat storage for solar DHW tanks. Mazman et al. [27] carried out experimental tests on a solar DHW tank of 150 l combined with three different PCM compounds, i.e. mixtures of paraffin and stearic acid (PS), paraffin and palmitic acid (PP), and stearic acid and myristic acid (SM) capsulated in a cylinder module at the top of the tank (similar to the PCM geometry used in [17, 18]). They concluded that PS gave the best results for thermal performance enhancement of the solar DHW tank with an efficiency of 74%. Kousksou et al. [28] conducted numerical study of PCM characteristics in solar-based DHW systems and showed that the high sensitivity of

the DHW system to the choice of first order design parameters such as the PCM melting temperature may open the perspective of successfully designing a PCM based DHW system that may be more efficient than its PCM free counterpart. While Padovan and Manzan [29] found the PCM had not the major impact on the results for the application system concerned through conducting genetic optimization on a PCM enhanced solar DHW tank for solar DHW systems using mono and multi-objective genetic algorithms. A further assessment for the benefit of PCMs in solar DHW systems done by Teamah et al. [30] showed that heat storage volume played a key role in influencing the collector performance and PCMs provided a benefit only in comparison to an undersized water based storage system. Besides, Fazilati and Alemrajabi [31] used a type of paraffin wax as a PCM in spherical capsules to enhance heat storage of solar water heater and observed that by using the PCM in the tank the energy storage density was increased in the tank up to 39% and the exergy efficiency was enhanced up to 16%.

Although there are lots of studies on DHW tanks as mentioned above, an appropriate solar heat storage tank module aimed to the low-temperature solar thermal market promotion is still necessary to be developed in particular with a cheap PCM as a thermal battery for shaking off peak auxiliary power or working under power outage. Most of the PCM heat storage tanks reported in the literature were not suitable for real engineering promotion. The present study considers a PCM heat storage tank manufactured by the H.M. Heizkörper Ltd. Company in Germany for DHW supply in

residential dwellings for the European low temperature solar thermal market. The PCM material is based on SAT (Sodium Acetate Trihydrate), which is essentially a form of salt and is cheap, circa 3-5 DKK/kg cost in current market. The investment cost of a tank containing 35 kg PCM on the basis of SAT has a slight cost increase neglecting few amount of additives for the SAT composite and the encapsulation cost of the tank. The specific composite components are unknown due to commercial confidentiality but more information can be referred to highly relevant work [32]. It is intended to design the solar DHW tank with good heat transfer matching properties meanwhile reducing heat mixing phenomena within the tank during charge and discharge, in order to make the tank module more cost-efficient. Lab tests of a prototype solar DHW tank and an improved tank were carried out to evaluate thermal performances of the tanks as well as heat content and stability of the PCM. Matching property design of the spirals in the solar DHW tank was discussed based on relevant tests. The improved tank was manufactured based on the test results of the prototype. Test results of the improved tank were adopted to verify the validity of the amelioration measures. Additionally, heat content of the PCM in the tank mantle was measured under a series of test cycles comprising charge and discharge to assess its capacity and stability.

2 Test facility and method

2.1 Designs of the prototype and the improved tanks

The solar heat storage tank design is intended to meet the DHW demands of a single family household combining solar heating with auxiliary heating. Bottom and top heat exchanger spirals are constructed in the tank for water circulations of solar and auxiliary heating, respectively. Figure 1 shows the tank structure (Thermal insulation layer is removed in Figure 1 (a)) and photos of the prototype and the improved tanks. Both tanks are composed of a stainless steel mantle with heat exchanger spirals, PCM, polyurethane (PUR) foam insulation as well as water draw-off pipes and pipe connections. The cold water entrance port located at the bottom side is elbowed into the tank bottom center, while the hot supply pipe is drawn from the tank top. For each tank, the inner volume is 148 l, excluding the volume of heat exchanger spirals. Tank height is 1.8 m and inner diameter is 356 mm. A weight of 35 kg PCM consisting of SAT composite is sealed in the mantle, with a thickness of 22 mm between the inner stainless steel mantle and the 90 mm PUR insulation material.

The main difference between the prototype and the improved tanks are the lengths of the spirals and the connection way of the hot supply pipes which will affect the matching properties and the thermal performance of the solar DHW tank, as listed in Table 1. The outer and inner diameters of the spirals are 20 and 18.5 mm, respectively. Design modification of the improved tanks is based on the testing analysis results of

the prototype tank, which will be elucidated in sections 3 and 4.

Figure 1 Schematic illustrations of the solar DHW tanks

Table 1. Configurations of the prototype tank and the improved tank

2.2 Test facility

Heat charge and discharge characteristics of both tanks are the matters of concern of the tests. As lab tests were considered instead of a practical application in a household, the simulated solar heating and auxiliary heating processes were achieved by an electrical heater available for 3 different power levels (3 kW, 6 kW, 9 kW). During the heat charges, a target temperature of 90 °C was set by the intelligent controller of the electrical heater to heat up the tank. Figure 2 gave the schematic diagram of the test facility, from which it could be seen that there were mainly two circulating loops in the test system, i.e. a closed-loop heat charge subsystem with two branches (solar charge and auxiliary charge) connected in parallel, as well as an open-loop DHW discharge subsystem. The simulated solar charge to the bottom spirals and the auxiliary charge to the top spirals were executed independently and separately by manual valve switches. It was therefore reasonable to adopt the same flowmeter to measure the flow rates of solar charge and auxiliary charge branches separately. Another flowmeter was installed at the tap water entry into the tank to measure the hot water draw-off flow rate during discharge. Temperatures of both loops at the inlet and outlet, as well as the ambient were monitored, along with the tank temperatures at

different vertical locations in the center, as illustrated in Figure 3. For the prototype tank, the thermocouple temperature sensors were evenly distributed. It was presumed through the test results that there was a temperature gradient near the tank bottom. Thus, three thermocouples were added at the tank bottom with a spacing of 0.05 m for the tests of the improved tank. Thermopiles were adopted to directly measure the temperature differences between the inlet and outlet of the heat charge and discharge loops, because temperature difference measured by the thermopiles was more accurate than that obtained by the remainder of measured inlet and outlet temperatures in light of the measuring principle.

Figure 2 Schematic diagram of the test facility

Figure 3 Location distributions of the thermocouple temperature sensors (a) for the prototype tank; (b) for the improved tank

All the data were recorded by a data logger system written in a LabView programming on a PC. Time interval of the data logger was 1 min. Figure 4 showed the pictures of the main test facility. Besides, all temperature sensors were Type K thermocouples made of copper/constantan with an accuracy level of ± 0.5 °C. Measuring error of the flowmeters was within 1% confirmed by weighting method calibrations.

Figure 4 Pictures of the heat storage test facility

2.3 Test conditions and calculating methods

For both tanks, a series of test cycles encompassing heat charge and discharge were undertaken to determine the steady-state tank heat loss coefficient, HXCRs of the top and bottom spirals, heat content of PCM, etc. A full test cycle represents a heat charge process followed with a heat discharge process.

To begin with, it is necessary to obtain the tank heat loss coefficient ($U_{tk,loss}$) through a long period of heat charge up to a steady-state heat loss with a low flow rate (about 1.0 l/min). The tank heat loss coefficient was determined by equation (1).

$$U_{tk,loss} = \frac{\dot{Q}}{\left(T_{tk,ave} - T_{amb}\right)} \tag{1}$$

where $T_{tk,ave}$ is the average tank water temperature and T_{amb} is the ambient temperature. The heat power $\dot{Q}$ for heat charge (also applies to heat discharge) is calculated by equation (2).

$$\dot{Q} = \dot{V} \cdot c_p \cdot \rho \cdot \left(T_{inlet} - T_{out}\right) \tag{2}$$

Where $\dot{V}$ is the volume flow rate of the heat transfer fluid measured at the inlet; c_p is the specific heat capacity of the heat transfer fluid; ρ is the density of the heat transfer fluid; T_{inlet} is the inlet temperature; T_{outlet} is the outlet temperature. Note that the temperature difference $\left(T_{inlet} - T_{outlet}\right)$ is directly measured by thermopiles.

The HXCR for the heat exchanger spirals indicates how fast heat can be transferred between the heat transfer fluid and the tank. A high HXCR is desired to fast charge the storage with a high power. The HXCR is expressed by the equation (3) [33].

$$HXCR = \dot{V} \cdot c_p \cdot \rho \cdot \ln \frac{\left(T_{inlet} - T_{tk,ave}\right)}{\left(T_{outlet} - T_{tk,ave}\right)} \quad (3)$$

To determine the HXCR of the bottom spiral, solar charge to the bottom spiral was implemented with a supply power of 3 kW, since the useful heat power got by a commonly used solar collector with an area of 3–4 m^2 was usually less than 3 kW. Solar charge to the bottom with flow rates of 4.6 l/min and 12 l/min lasting for 6 h were executed separately for the prototype tank, and it was found that HXCR of the bottom spiral can be obtained at a higher flow rate (12 l/min) due to the fact that the outlet temperature of the spiral was very close to the average tank temperature. When it came to measure the HXCR of the top spiral for auxiliary charge, supply powers of both 3 kW and 9 kW were considered with a high flow rate (above 13 l/min) to show the dependence of HXCR on different supply powers. When the tank top temperature achieved 50 °C the auxiliary charge was stopped.

In determining the heat content contribution of the PCM, solar charge with a long stability period (more than 2 days) at a high tank temperature (82–86 °C) was started with a uniform tank temperature, followed by a long DHW discharge of several days to identify the full heat discharge. And a series of test cycles were implemented for

both tanks in order to assess the PCM heat capacity and indirectly infer the stability of the PCM. The change of heat content in the tank over a specific charge time period was determined by equation (4), which also applied to the calculation of heat discharge power.

$$\Delta Q_{charge}(\tau) = \int_0^{\tau} \left[\dot{Q} - U_{tk,loss}\left(T_{tk,ave} - T_{amb}\right)\right] \cdot d\tau \tag{4}$$

For the solar charge from initial state to the end, thermal balance was given by equation (5).

$$\int_0^{\tau} \left[\dot{Q} - U_{tk,loss}\left(T_{tk,ave} - T_{amb}\right)\right] \cdot d\tau = \int_0^{\tau} \left(\rho c_p V_{tk} + (\rho c_p)_{steel} V_{spirals}\right) \cdot \left(T_{inlet} - T_{outlet}\right) \cdot d\tau + Q_{PCM} \tag{5}$$

where V_{tk} is the tank water volume; $(\rho c_p)_{steel}$ is the product of density and specific heat capacity for common stainless steel; $V_{spirals}$ is the volume of the spirals; Q_{PCM} is the heat content of the PCM in the temperature interval between the initial and end states.

3 Test results and analysis of the prototype DHW tank

In the first test cycle of the prototype tank, a solar charge of 30 h was done to attain a steady-state heat loss with a low flow rate of 1.3 l/min. Tank heat loss coefficient of 2.7 W/K was obtained for the prototype tank at a tank temperature of 84.5 °C.

3.1 Matching property of the bottom spiral for solar charge

Solar charge of 6 h with a supply power of 3 kW was conducted at a flow rate of 4.6 l/min in order to determine HXCR of the bottom spiral of the prototype tank. However, it was found that calculations of HXCR by equation (3) didn't make sense due to the fact that the outlet temperature of the spiral was very close to the average tank temperature under a lower flow rate. It was assumed that solar charge with a higher flow rate would attain a higher spiral outlet temperature than the tank temperature. Therefore, another solar charge with a flow rate of 12 l/min was taken after the previous test cycle. Figures 5 and 6 showed the temperature development during solar charge and the HXCR of the bottom spiral, respectively, with a flow rate of 12 l/min. From Figure 5 there seemed to be no thermal stratification during charge, as there was no temperature sensor below 0.3 m height where thermal stratification most likely appeared (Regarding the temperature locations please see Figure 3(a)). It was found that the HXCR of the bottom spiral varied from 960 to 2000 W/K, excluding the measuring values after 4 h because those measuring values were reckoned to be inaccurate when the spiral outlet temperature approached to the average tank temperature.

Figure 5 Temperature development of the prototype tank during solar charge

Figure 6 HXCR of the bottom spiral of the prototype tank with a flow rate of 12 l/min

For a typical conventional solar DHW tank, an empirical mass flow rate ($\dot{m}_f$) of 0.75

l/min per m^2 collector (equivalent to 0.012 kg/(s m^2)) is recommended in real engineering for a commonly used solar collector. Thus the heat transport capacity rate per m^2 solar collector corresponds to $c_p \dot{m}_f$ = 4190 [J/kg K]*0.012 [kg/(s m^2)] = 50 W/(m^2 K). To maximize cost-efficiency of the tank, it is desired that the HXCR of the bottom heat exchanger spiral matches with the heat transport capacity rate of the solar collector. A commonly used solar collector with an area of 3–4 m^2 is recommended for a solar DHW tank in real engineering according to the hot water demands of a typical single family household. It means that the heat transport capacity rate of a commonly used solar collector is 150–200 W/K. However, the measured HXCR of 960–2000 W/K for the bottom spiral corresponds to 20–40 m^2 solar collectors. It indicates that the bottom heat exchanger spiral with a length of 28 m is strongly oversized, resulting in a poor matching property between the heat exchanger spiral and a commonly used solar collector.

3.2 Matching property of the top spiral for auxiliary charge

For the auxiliary charge, supply powers of both 3 kW and 9 kW were considered to determine the HXCR of the top spiral of the prototype tank with flow rates of 13.3 l/min and 13.8 l/min, respectively for the two cases. The auxiliary charges were stopped when the tank top temperature achieved 50 °C. Figure 7 shows the temperature developments for both cases. Figure 8 gives the HXCR of the top spiral of the prototype tank for the two supply power levels. The HXCR is dependent on the

supply power and water tank temperature. The HXCR of the top spiral with the supply power of 3 kW is in the rage of 195–340 W/K, while that with the supply power of 9 kW varies over the range of 251 W/K to 372 W/K. Except a faster heating process for 9 kW supply power in Figure 7, only a small increase of HXCR for 9 kW supply power is observed compared to the case of 3 kW supply power. In [34] a design rule for auxiliary heat exchanger spirals connected to burners/boilers is given as:

The power of the burners/boilers must not be larger than:

$$(22[K] \cdot \text{Heat exchange capacity rate of spiral } [W/K]) + \left(\frac{\text{Water volume in heat exchange spiral loop } [L] \cdot 1000\ [W]}{4.5\ [L]}\right)$$

Based on the rule of thumb the top spiral is only suitable for boiler up to about 8 kW. Whilst the supply power of a commonly used boiler for household DHW is about 20 kW, which indicates a mismatch of supply power for auxiliary charge and the top spiral with a length of 7 m is undersized. It is therefore recommended to increase the length of the top spiral. Figure 9 shows the recommended lengths for the heat exchanger spirals in the top of the tank as a function of the boiler power [35]. According to Figure 9, it is inferred that the length of the top spiral should be above 17 m.

Figure 7 Auxiliary charge to the top spiral of the prototype tank with a flow rate above

13 l/min

Figure 8 HXCR of the top spiral of the prototype tank versus top tank temperature

Figure 9 Recommended lengths for the heat exchanger spirals in the top of the tank as a function of the boiler power

3.3 Characteristic of heat discharge for the prototype tank

Figure 10 delineates the temperature development during hot water draw-off of 180 l with a flow rate of 10 l/min. The heat discharge was started from the end of a solar charge process of 6.6 h. Initial temperature of discharge for the tank was 85.7 °C. It was found that the hot supply temperature decreased linearly during the period of a draw-off volume of 148 l (around 15 min). The maximum temperature difference between the hot water supply pipe and the top tank temperature appeared near a full discharge of the water tank volume. When a full discharge at a flow rate of 5 l/min was undertaken, the maximum temperature decrease nearly doubled as the discharge time doubled compared to the case of 10 l/min. It was presumed that the decrease of the hot supply temperature within 15 min after discharge start (see Figure 10) was due to the heat transfer between the stainless steel water supply pipe and tank water at the lower part. Figure 11 illustrated the schematic sketch of heat mixing through the wall of hot supply pipe. It was therefore suggested to replace the stainless steel pipe with a PEX plastic pipe with a thick wall or revise the connection way of the hot water supply pipe to avoid heat mixing and obtain a hot water supply temperate as close as

the top tank temperature.

Figure 10 Temperature development of the prototype tank during hot water draw-off of 180 l with a flow rate of 10 l/min

Figure 11 Schematic sketch of heat mixing through the wall of hot supply pipe

3.4 Heat content and stability of the PCM in the prototype tank mantle

The PCM on the basis of SAT in the tank mantle acts as a thermal battery which enables to store more energy. The heat content of the PCM was assessed for a series of test cycles. Table 2 gave the heat content assessment of the PCM in the prototype tank under a series of test cycles compared to the ideally working SAT (the thermophysical properties of which was referred to [32]). It indicated that the PCM heat content was somewhat lower than that of ideally working SAT. Meanwhile, it could be inferred that the PCM was stable without phase segregation under a series of test cycles according to the estimation results, as no performance degradation was found with 16 test cycles lasting for more than 3 months. And no supercooling condition was found for the prototype.

Table 2. Heat content of the PCM under a series of test cycles for the prototype tank

4 Test results of the improved tank and verification of the amelioration measures

According to the test results of the prototype tank, the bottom spiral for solar charge was strongly oversized, while the top spiral for auxiliary charge was undersized. Additionally, the hot supply pipe should be replaced by a PEX plastic pipe with a thick wall or the connection way of the hot supply pipe should be revised to avoid heat mixing. The improved tank was made by cutting down the bottom spiral length to 22.5 m and increasing the top spiral length to 20.4 m, as already mentioned in Table 1. Meanwhile, the hot supply pipe was revised to directly draw off hot water from the top via a pipe connection buried in the PUR insulation layer, as shown in Figure 12. Consequently, the insulation layer of the improved tank was somewhat different from the prototype as shown in Figure 1 (b) and (c). Tank heat loss coefficient of the improved module was measured to be 2.6 W/K at an average tank temperature of 85.3 °C. It indicated that the tank heat loss was close to that of the prototype.

Figure 12 Schematic sketch of the hot supply pipe drawing off water from the top via a pipe connection buried in the insulation layer for the improved tank

4.1 Matching property and appropriate length of the bottom spiral

Solar charge over a period of 50 h was carried out with a flow rate of 12.3 l/min for the improved tank. Figure 13 shows the temperature development during the charge of 10 h since it approaches steady state after 10 h (for the temperature sensor locations

please see Figure 3(b)). Comparing with the solar charge of the prototype in Figure 5, the outlet water temperature of the solar charge for the improved tank is evidently higher than the tank temperatures before 6 h. This is mainly because the bottom spiral length is reduced and corresponding HXCR decreases. A visible temperature gradient is found at the bottom of the tank as shown in Figure 14, since four thermocouples (T7-T10, see Figure 3(b)) have been buried in the lower locations. While for the prototype no thermal stratification has been found because no thermocouple is considered below 0.3 m height. Figure 15 gives the HXCR during the solar charge. The measured HXCR is in the range of 500–1000 W/K, corresponding to 10–20 m^2 solar collectors in terms of the heat transport capacity rate of 50 W/K per m^2 solar collector. It means that the bottom spiral is still oversized.

Figure 13 Temperature development of the improved tank during solar charge with a flow rate of 12.3 l/min

Figure 14 Temperature distribution of the improved tank during solar charge

Figure 15 HXCR of the bottom spiral of the improved tank with a flow rate of 12.3 l/min

To estimate the appropriate length for the bottom spiral, the comprehensive heat transfer coefficient of the measured heat exchanger spirals is separated from the HXCR, which represents the product (KA) of the comprehensive heat transfer coefficient (K) and corresponding heat transfer area (A) of the spiral. As the outer

diameter of the spirals is 20 mm, it is easy to obtain the comprehensive heat transfer coefficients for specific spirals. Figure 16 delineates the comprehensive heat transfer coefficients of the heat exchanger spirals at different lengths, i.e. 28 m bottom spiral and 7 m top spiral for the prototype tank as well as 22.5 m bottom spiral for the improved tank. It indicates that the comprehensive heat transfer coefficient is dependent upon the spiral length and water tank temperature. A longer spiral length will give rise to a higher comprehensive heat transfer coefficient. Meanwhile, the comprehensive heat transfer coefficient enhances as the water tank temperature increases.

Figure 16 Comprehensive heat transfer coefficients of the heat exchanger spirals at different lengths.

Although the case of the top spiral is different from that of the bottom spiral due to their locations within the tank, it can provide a reference to assess the comprehensive heat transfer coefficients of different lengths. Once the water tank temperature is chosen, the comprehensive heat transfer coefficients for various spiral lengths can be estimated by interpolation. In the present study, a moderate temperature of 50 °C in Figure 16 is chosen as the typical water tank temperature. Thus the appropriate spiral length can be obtained through a simple iterative process using equation (6). Specifically, assume an initial length value (L) between 7 m and 22.5 m and get the comprehensive heat transfer coefficient (K) at 50 °C via interpolation to calculate the

revised length (L^*). Then make the iterative process until the assumed length value is the same as the revised length. Through iteration, the appropriate lengths for the bottom spiral with HXCRs of 150 and 200 W/K are 9 m and 11.3 m respectively, considering comprehensive heat transfer coefficients of 266 W/(m^2 K) and 282 W/(m^2 K) at 50 °C, respectively, for the two spiral lengths.

$$HXCR = K \cdot \pi \cdot d \cdot L \qquad \text{(150–200 W/K for 3–4 m}^2\text{ solar collector)} \qquad (6)$$

Where K is the comprehensive heat transfer coefficient; d is the outer diameter of the spiral; L is the length of the spiral.

4.2 Matching property of the top spiral for the improved tank

Figure 17 shows the HXCRs of the top spiral with auxiliary charge with two different supply power levels. HXCR of the top spiral with supply powers of 3 kW and 9 kW are in the ranges of 510–1010 W/K and 670–1070 W/K, respectively. The top spiral with a length of 20.4 m is found to be suitable for boilers up to a power of 23.6 kW according to the case of 9 kW power supply and the rule of thumb stated in Section 3.2. It suggests that the matching property of the top spiral for the tank is improved.

Figure 17 HXCR of the top spiral of the improved tank with a flow rate of 13.8 l/min

4.3 Characteristic of heat discharge for the improved tank

Figure 18 delineates the temperature development of the improved tank during hot water draw-off of 180 l with a flow rate of 10 l/min starting from the end of a long charge of 50 h. The hot water supply temperature of the improved tank is nearly the same as the top tank temperature, which means heat is not transferred downwards in the tank during discharge. It indicates that the connection modification of the hot supply pipe shown in Figurer 12 enables to avoid heat mixing during hot water draw-offs, giving rise to a high quality of hot water supply.

In view that the Stratification number [3, 4], which represents the ratio of the mean of the transient temperature gradients to the maximum mean temperature gradient, can effectively evaluate the thermal behavior of a storage tank during heat charge and discharge, it is used to characterize the thermal stratification degree of the prototype and the improved tanks during discharge. Figure 19 makes the comparison of the Stratification numbers for both tanks with flow rates of 5 l/min and 10 l/min, respectively. It seems that the thermal stratification of the improved tank is superior to that of the prototype regardless of the initial effect.

Figure 18 Temperature development of the improved tank during hot water draw-off of 180 l with a flow rate of 10 l/min

Figure 19 Comparison of the Stratification numbers for the prototype and the improved tanks

4.4 Heat content and contribution of PCM for the improved tank

Table 3 gives the heat content assessment of the PCM under a couple of test cycles for the improved version. Test cycle No.1 was presumed to go through supercooling according to the results of test cycle No. 2. Comparing the ratios of the measured PCM heat content to the theoretical heat content of ideally working SAT in Table 3 with Table 2, it was found that the ratios in the former were a little bit lower than those in the latter, suggesting that the PCM contribution of the improved tank was somewhat decreased compared to the prototype mainly due to spiral heat transfer effect (a smaller HXCR of the bottom spiral for the improved version).

Table 3. Heat content of the PCM under a couple of test cycles for the improved version

Moreover, a specific test cycle is used to determine the efficiency of the PCM. Solar charge of a long stability period (50 h) is considered for the full charge of PCM. Accumulated heat charging quantity of the tank & steel (steel spirals in the tank) over the period of 0.25 h–10 h by measurement is 12.37 kWh (±0.02 kWh) according to thermal enthalpy difference. The initial 0.25 h has been excluded from the heat capacity accumulation due to an initial non-equilibrium heat transfer from the power heater to the inner of the tank. Meanwhile, accumulated heat charging quantity of the PCM over the period is 3.82 kWh (±0.02 kWh) in a temperature interval of 17.3–87.3 °C. It suggests that heat content of the PCM accounts for 24% of total heat

charging quantity in the temperature interval.

For the heat discharge, it is observed that heat released by the PCM during discharge with tank temperature decreasing from 87.3 °C to 16 °C (achieving a steady-state end) is 2.7 kWh. Approximately, 70.7% of the PCM heat storage contributes to the tank water.

5 Conclusions

Lab tests of a prototype solar DHW tank and an improved version with a water volume of 148 l and 35 kg PCM in the mantle were carried out to evaluate thermal performances of the tanks and heat content of the PCM during heat charge and discharge. The PCM on the basis of cheap SAT was considered as a thermal battery for shaving off peak auxiliary power or working under power outage. Tests of the prototype tank module showed that there were some technical problems, such as mismatching property of the heat exchanger spirals (heavily oversized for the bottom spiral and undersized for the top spiral), heat mixing phenomena during hot water draw-off. The improved tank module manufactured by according amelioration measures based on the test results of the prototype was further tested to verify the improvement. It was found that the matching property of the top heat exchanger spiral was ameliorated for auxiliary charge and the heat mixing between hot water supply pipe and water tank was restrained during discharge, except the length of the bottom spiral should be further reduced to 9–11.3 m (considering a commonly used collector

with an area of 3–4 m^2).

Regarding the PCM in the mantle, it was inferred that the PCM heat content was somewhat lower than that of ideally working SAT. About 70.7% of the PCM heat storage contributed to the tank water. Furthermore, the PCM composite tended to be stable without performance degradation according to the assessment of 16 test cycles lasting for more than 3 months. It indicated that the PCM heat storage worked well as a thermal battery and would be a potential for promotion in domestic heat storage of dwellings in the low-temperature solar thermal market.

Acknowledgment

The authors would like to thank the H.M. Heizkörper Ltd. Company in Germany for providing the testing water tank modules. And Jie Deng was thankful for the National Natural Science Foundation of China (Grant No. 51506193).

References

[1] S. Furbo, Using water for heat storage in thermal energy storage (TES) systems, In: Cabeza LC (Ed.), *Advances in Thermal Energy Storage Systems: Methods and Applications*, A volume in Woodhead Publishing Series in Energy (2015) 31-47.

[2] S. Furbo and E. Andersen, Heat storage for solar heating system – Now and in the

future, In: *Proceedings of Conference on Thermal Storage*, Prague, Czech Republic, 2008.

[3] J. Fernández-Seara, F.J. Uhía, J. Sieres, Experimental analysis of a domestic electric hot water storage tank, Part II: dynamic mode of operation, Applied Thermal Engineering 27 (2007) 137–144.

[4] O. Abdelhak, H. Mhiri, P. Bournot, CFD analysis of thermal stratification in domestic hot water storage tank during dynamic mode, Building Simulation 8 (2015) 421–429.

[5] P. González-Altozano, M. Gasque, F. Ibáñez, et al., New methodology for the characterisation of thermal performance in a hot water storage tank during charging, Applied Thermal Engineering 84 (2015) 196–205.

[6] A. Castell, M. Medrano, C. Sole, et al., Dimensionless numbers used to characterize stratification in water tanks for discharging at low flow rates, Renewable Energy 35 (2010) 2192–2199.

[7] I.J. Moncho-Esteve, M. Gasque, P. González-Altozano, G. Palau-Salvador, Simple inlet devices and their influence on thermal stratification in a hot water storage tank, Energy and Buildings 150 (2017) 625–638.

[8] E. Andersen, S. Furbo, M. Hampel, et al., Investigations on stratification devices for hot water heat stores, International Journal of Energy Research 32 (2008) 255–263.

[9] J. Dragsted, S. Furbo, M. Dannemand, F. Bava, Thermal stratification built up in hot water tank with different inlet stratifiers, Solar Energy 147 (2017) 414–425.

[10] Z. Wang, H. Zhang, B. Dou, et al., The thermal stratification characteristics affected by a novel equalizer in a dynamic hot water storage tank, Applied Thermal Engineering 126 (2017) 1006-1016.

[11] A. Zachár, Investigation of a new helical flow distributor design to extract thermal energy from hot water storage tanks, International Journal of Heat and Mass Transfer 80 (2015) 844–857.

[12] J. Fan, S. Furbo, Thermal stratification in a hot water tank established by heat loss from the tank, Solar Energy 86 (11) (2012) 3460–3469.

[13] J. Fan, S. Furbo, Buoyancy driven flow in a hot water tank due to standby heat loss, Solar Energy 86 (11) (2012) 3438–3449.

[14] C.A. Cruickshank, S.J. Harrison, Heat loss characteristics for a typical solar domestic hot water storage, Energy and Buildings 42 (2010) 1703–1710.

[15] L.F. Cabeza, M. Ibáñez, C. Solé, et al., Experimentation with a water tank including a PCM module, Solar Energy Material & Solar Cells 90 (2006) 1273–1282.

[16] M. Nabavitabatabayi, F. Haghighat, A. Moreau, P. Sra, Numerical analysis of a thermally enhanced domestic hot water tank, Applied Energy 129 (2014) 253–260.

[17] D.N. Nkwetta, P.E. Vouillamoz, F. Haghighat, et al., Phase change materials in hot water tank for shifting peak power demand, Solar Energy 107 (2014) 628–635.

[18] A. Najafian, F. Haghighat, A. Moreau. Integration of PCM in domestic hot water

tanks: Optimization for shifting peak demand, Energy and Buildings 106 (2015) 59–64.

[19] S. Furbo, Low flow solar heating systems, Educational note U-067, Department of Civil Engineering, Technical University of Denmark, Kgs. Lyngby, Denmark, 2004.

[20] W. Duff, Advanced solar domestic hot water systems, A report of the Task 14 Advanced Solar Domestic Hot Water Systems Working Group, IEA International Energy Agency Solar Heating and Cooling Programme, 1996.

[21] S. Knudsen, S. Furbo, Thermal stratification in vertical mantle heat-exchangers with application to solar domestic hot water systems, Applied Energy 78 (2004) 254–272.

[22] S. Furbo, S. Knudsen, Improved design of mantle tanks for small low flow SDHW systems, International Journal of Energy Research 30 (12) (2006) 955–965.

[23] A.A. Dehghan, A. Barzegar, Thermal performance behavior of a domestic hot water solar storage tank during consumption operation, Energy Conversion and Management 52 (1) (2011) 468–476.

[24] M. Arslan, A.A. Igci, Thermal performance of a vertical solar hot water storage tank with a mantle heat exchanger depending on the discharging operation parameters, Solar Energy 116 (2015) 184–204.

[25] L.J. Shah, S. Furbo, Entrance effects in solar hot water stores, Solar Energy 75 (4) (2003) 337–348.

[26] U. Jordan, S. Furbo, Thermal stratification in small solar domestic storage tanks caused by draw-offs, Solar Energy 78 (2) (2005) 291–300.

[27] M. Mazman, L.F. Cabeza, H. Mehling, et al., Utilization of phase change materials in solar domestic hot water systems, Renewable Energy 34 (2009) 1639–1643.

[28] T. Kousksou, P. Bruel, G. Cherreau, et al., PCM storage for solar DHW: from an unfulfilled promise to a real benefit, Solar Energy 85 (2011) 2033–2040.

[29] R. Padovan, M. Manzan, Genetic optimization of a PCM enhanced storage tank for Solar Domestic Hot Water Systems, Solar Energy 103 (2014) 563–573.

[30] H.M. Teamah, M.F. Lightstone, J.S. Cotton, An alternative approach for assessing the benefit of phase change materials in solar domestic hot water systems, Solar Energy 158 (2017) 875-888.

[31] M.A. Fazilati, A.A. Alemrajabi, Phase change material for enhancing solar water heater, an experimental approach, Energy Conversion and Management 71 (2013) 138–145.

[32] M. Dannemand, J. B. Johansen, S. Furbo, Solidification behavior and thermal conductivity of bulk sodium acetate trihydrate composites with thickening agents and graphite, Solar Energy Materials and Solar Cells 145 (2016) 287-295.

[33] M. Dannemand, W. Kong, J.B. Johansen, S. Furbo, Laboratory Test of a Cylindrical Heat Storage Module with Water and Sodium Acetate Trihydrate, Energy Procedia 91 (2016) 122-127.

[34] S. Furbo, Heat storage for solar heating system, Educational Note U-071, ISSN

1396-4046, Department of Civil Engineering, Technical University of Denmark, Kgs. Lyngby, Denmark, 2005.

[35] S. Furbo, Hot water tanks for solar heating systems, Report No. R-100, Department of Civil Engineering, Technical University of Denmark, Kgs. Lyngby, Denmark, 2004.

Table Captions:

Figure Captions:

Figures:

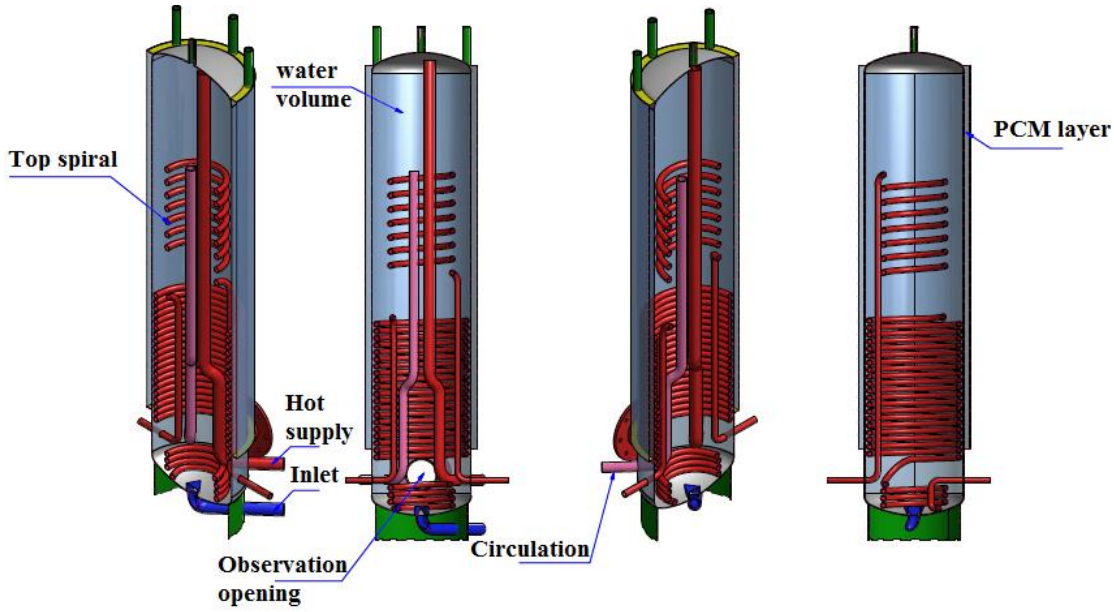

(a) Structure of the solar DHW tank

(b) Photo of the prototype tank

(c) Photo of the improved tank

Figure 1 Schematic illustrations of the solar DHW tanks

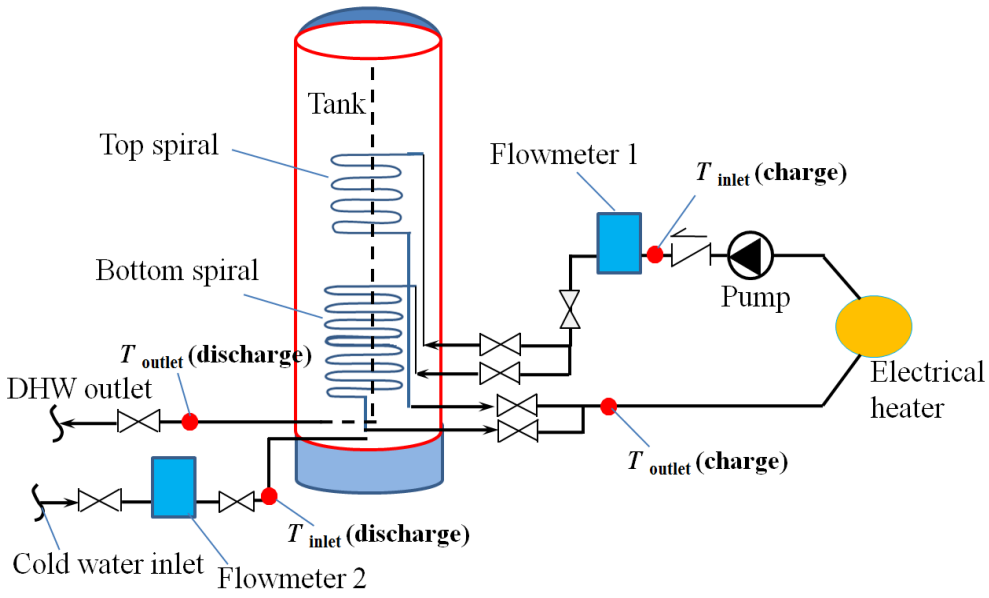

Figure 2 Schematic diagram of the test facility

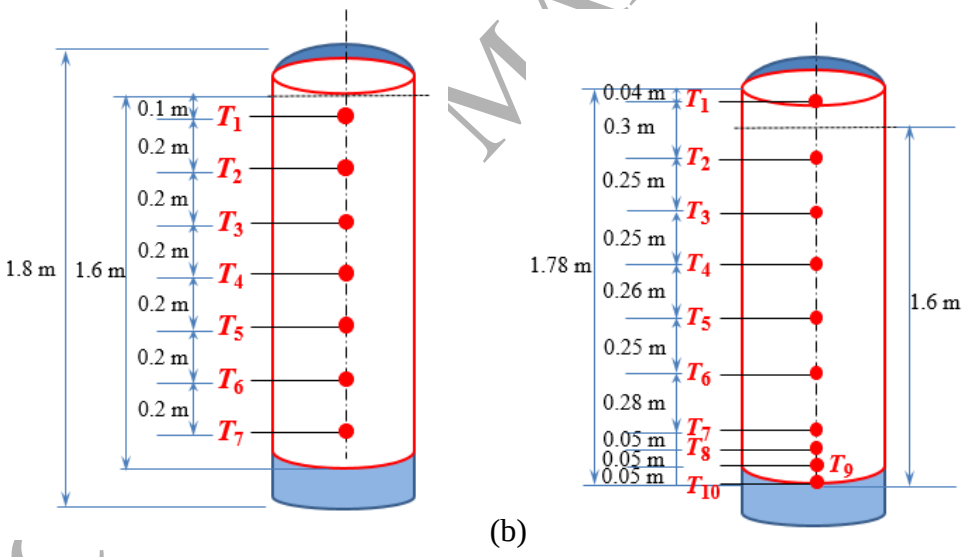

(a) (b)

Figure 3 Location distributions of the thermocouple temperature sensors (a) for the prototype tank; (b) for the improved tank

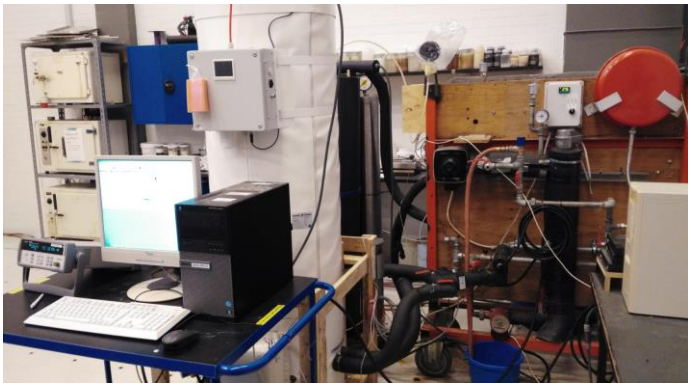

(a) Heat storage test facility used for the tests

(b) Electrical heater for simulated power supply

(c) Flowmeter installed in the heat charging loop

(d) Inlet, outlet and valves of DHW system

Figure 4 Pictures of the heat storage test facility

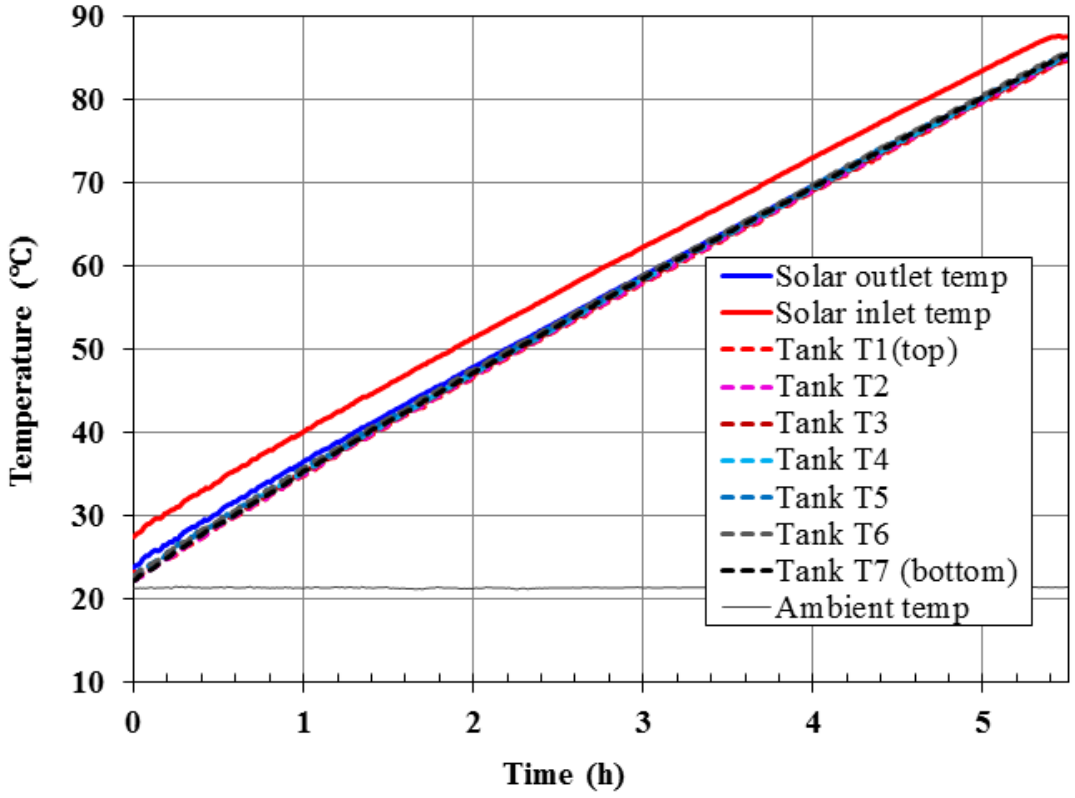

Figure 5 Temperature development of the prototype tank during solar charge

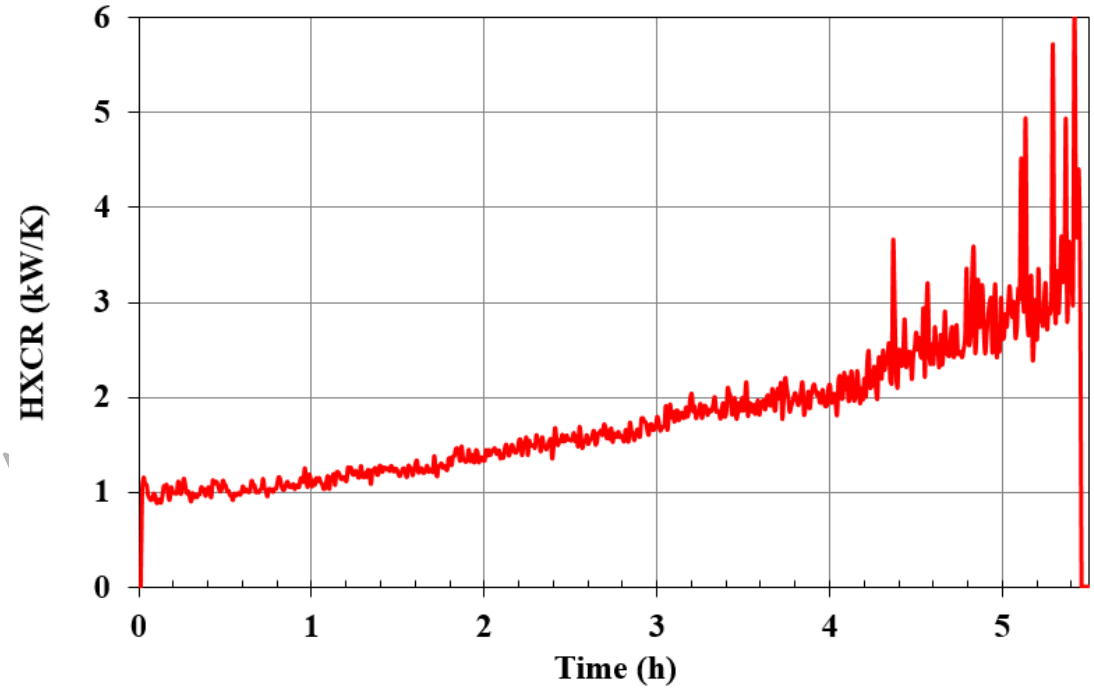

Figure 6 HXCR of the bottom spiral of the prototype tank with a flow rate of 12 l/min

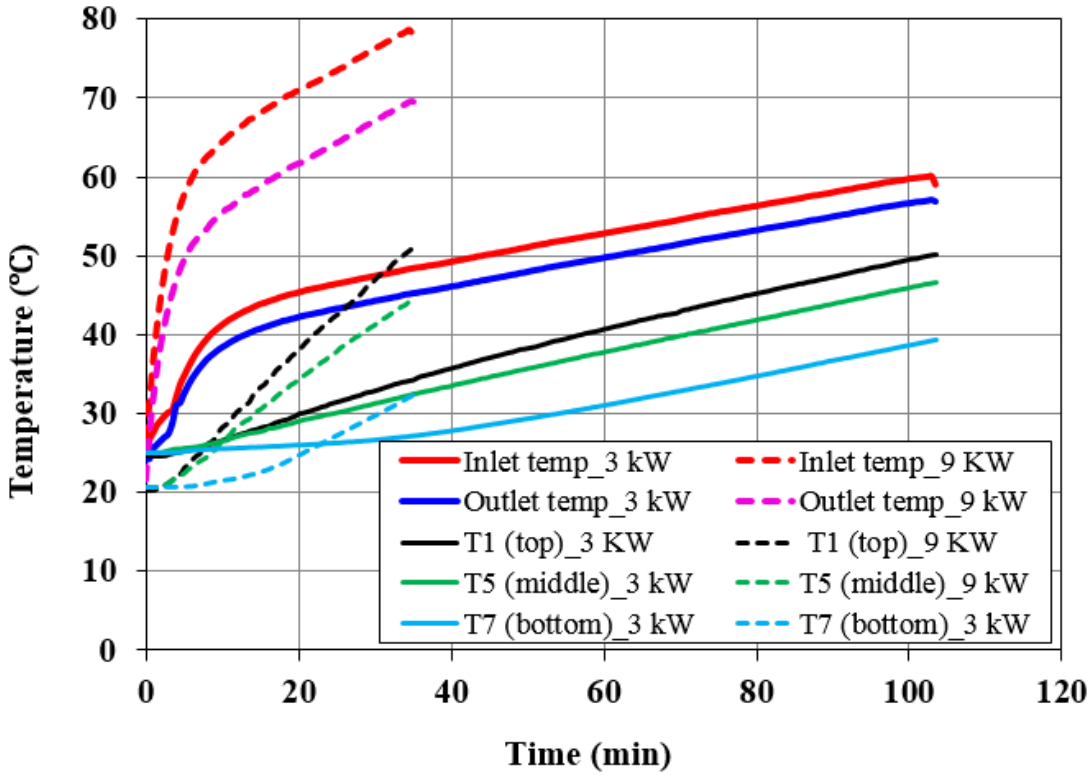

Figure 7 Auxiliary charge to the top spiral of the prototype tank with a flow rate above 13 l/min

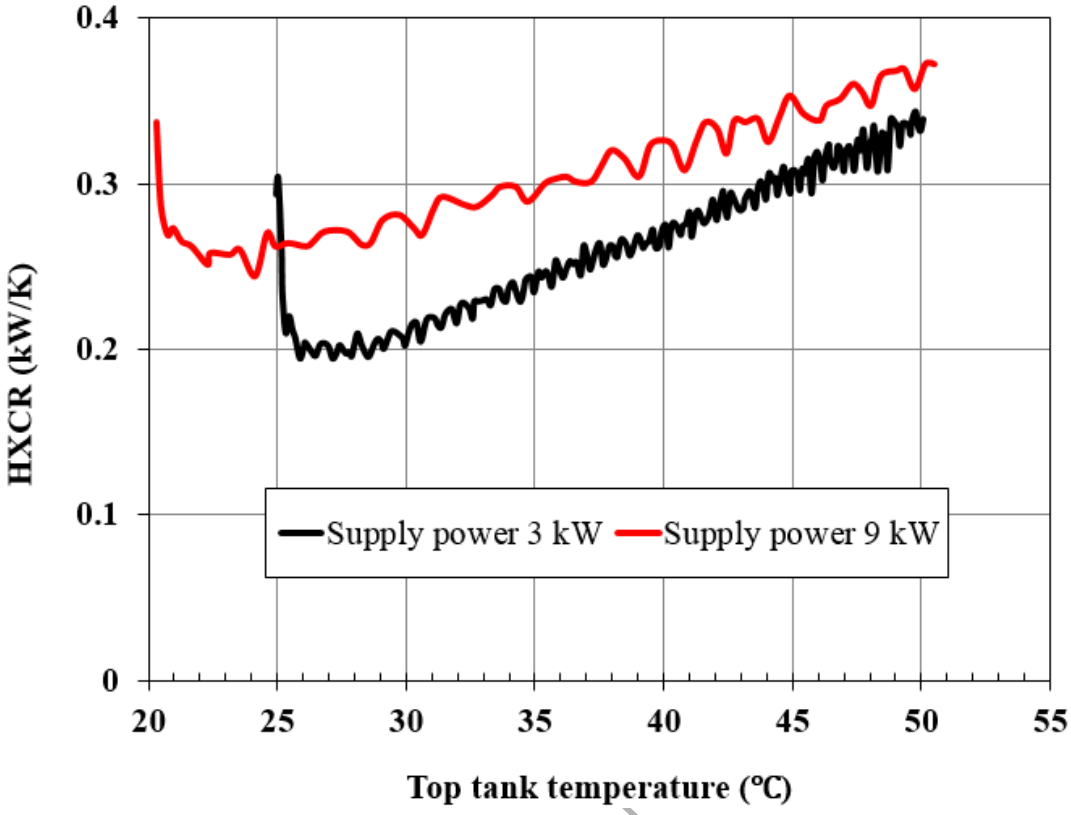

Figure 8 HXCR of the top spiral of the prototype tank versus top tank temperature

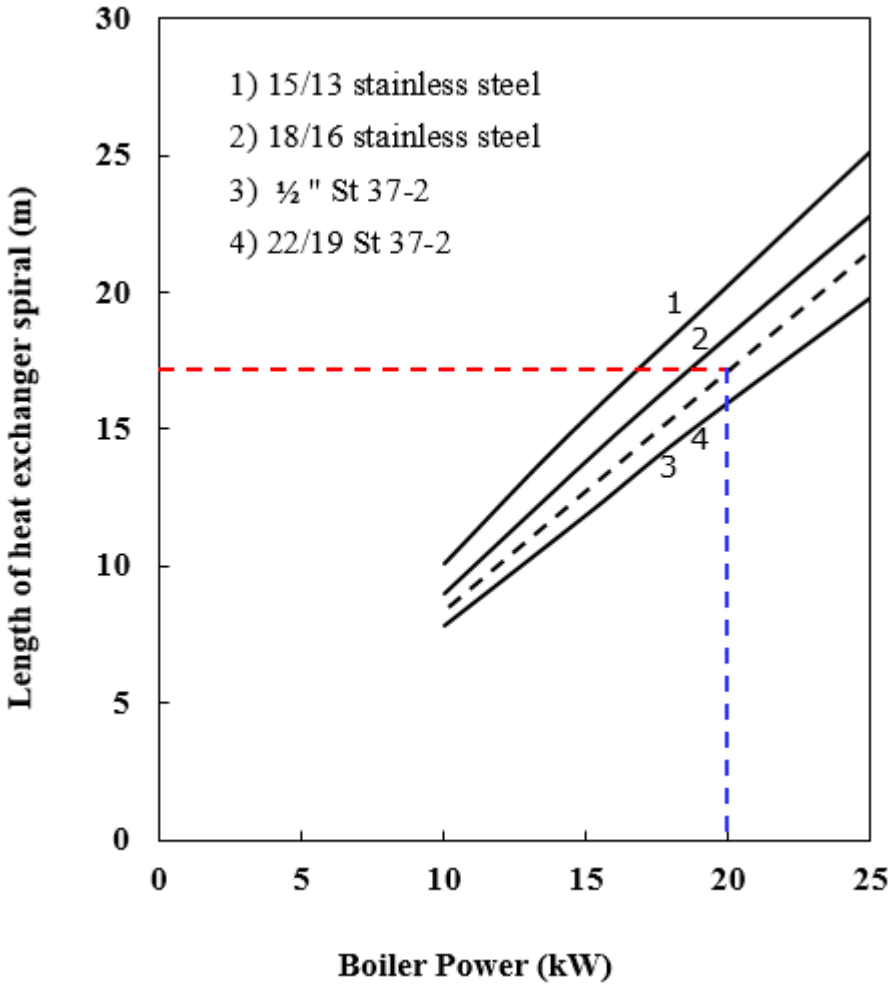

Figure 9 Recommended lengths for the heat exchanger spirals in the top of the tank as a function of the boiler power

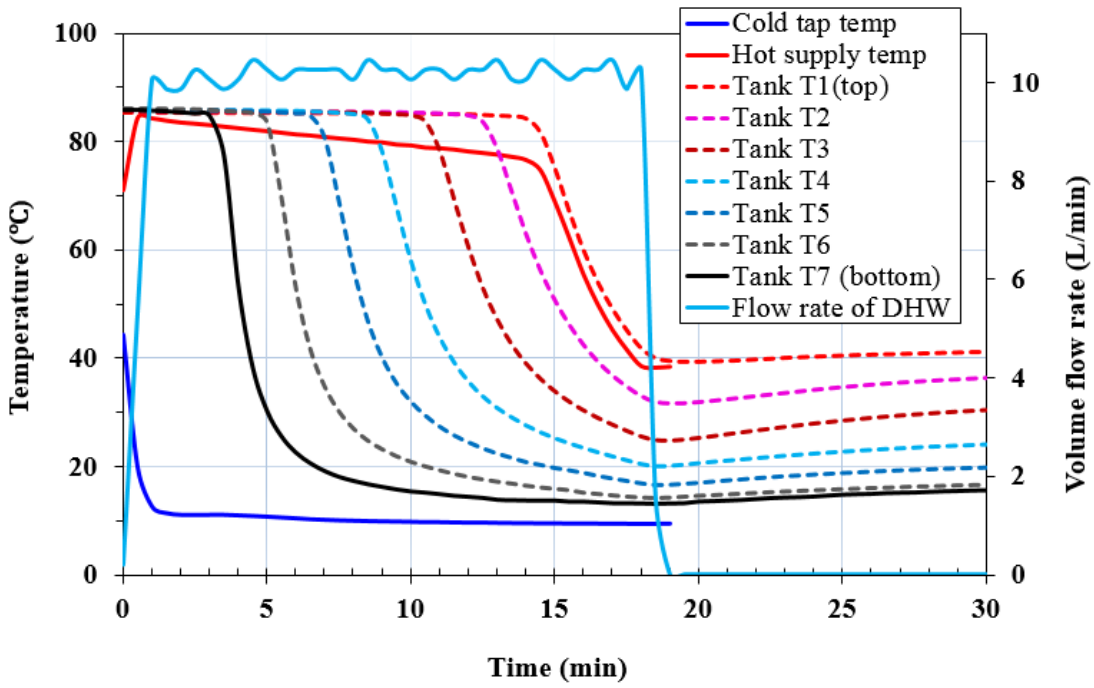

Figure 10 Temperature development of the prototype tank during hot water draw-off of 180 l with a flow rate of 10 l/min

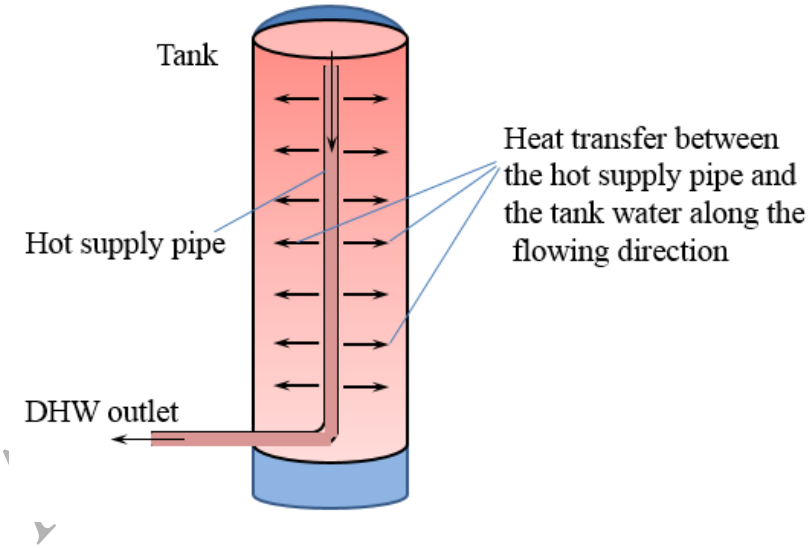

Figure 11 Schematic sketch of heat mixing through the wall of hot supply pipe

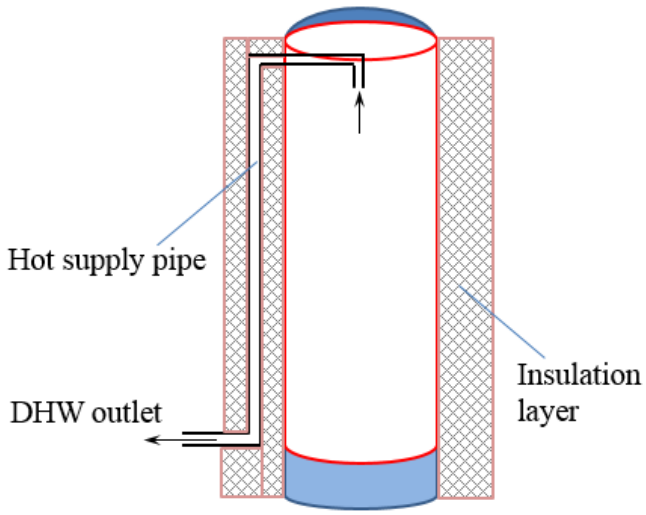

Figure 12 Schematic sketch of the hot supply pipe drawing off water from the top via a pipe connection buried in the insulation layer for the improved tank

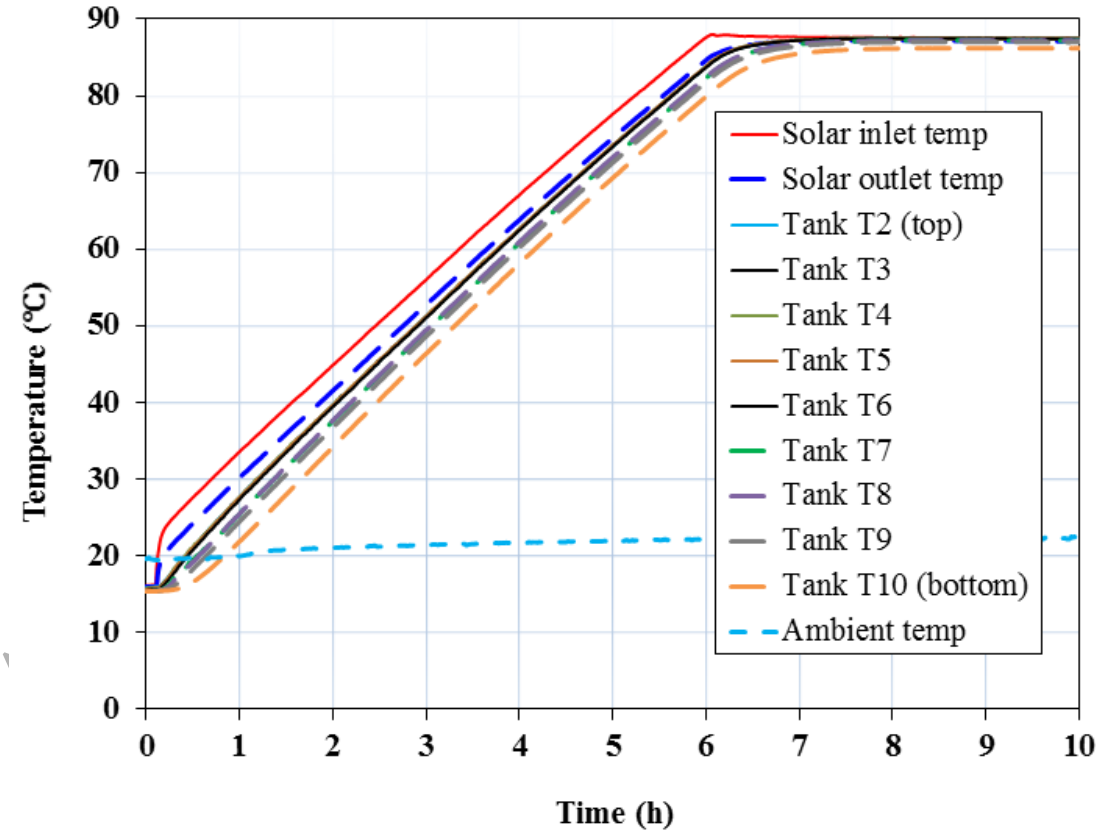

Figure 13 Temperature development of the improved tank during solar charge with a flow rate of 12.3 l/min

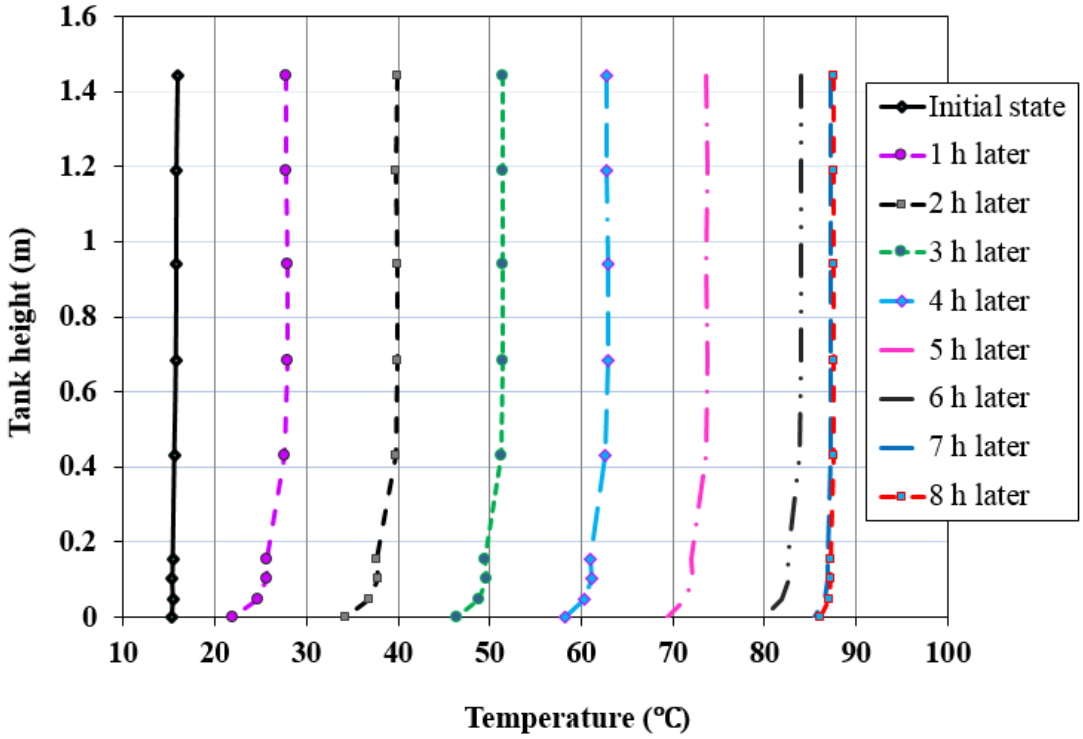

Figure 14 Temperature distribution of the improved tank during solar charge

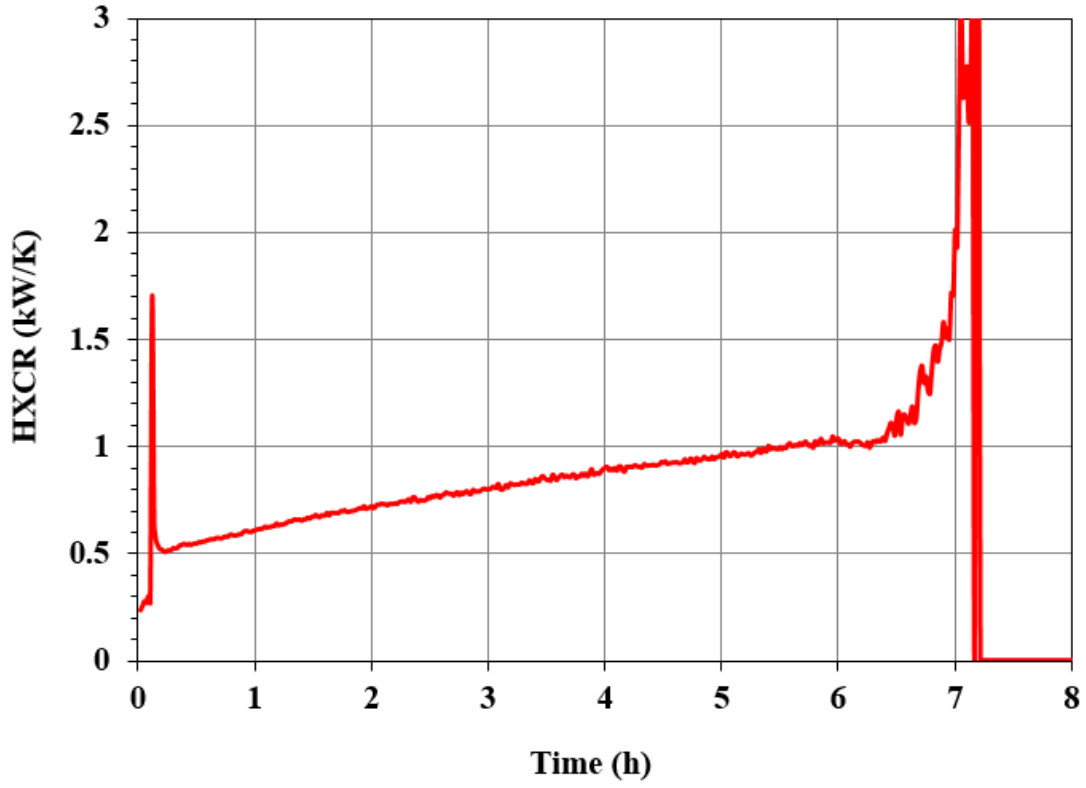

Figure 15 HXCR of the bottom spiral of the improved tank with a flow rate of 12.3 l/min

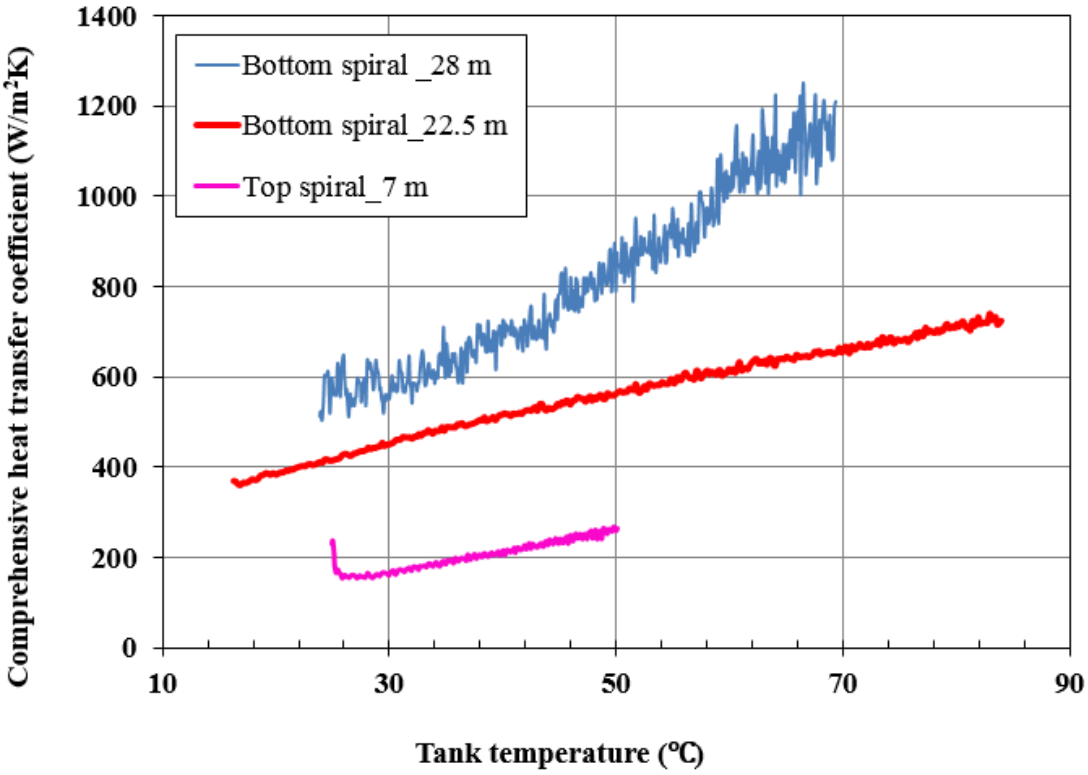

Figure 16 Comprehensive heat transfer coefficients of the heat exchanger spirals at different lengths

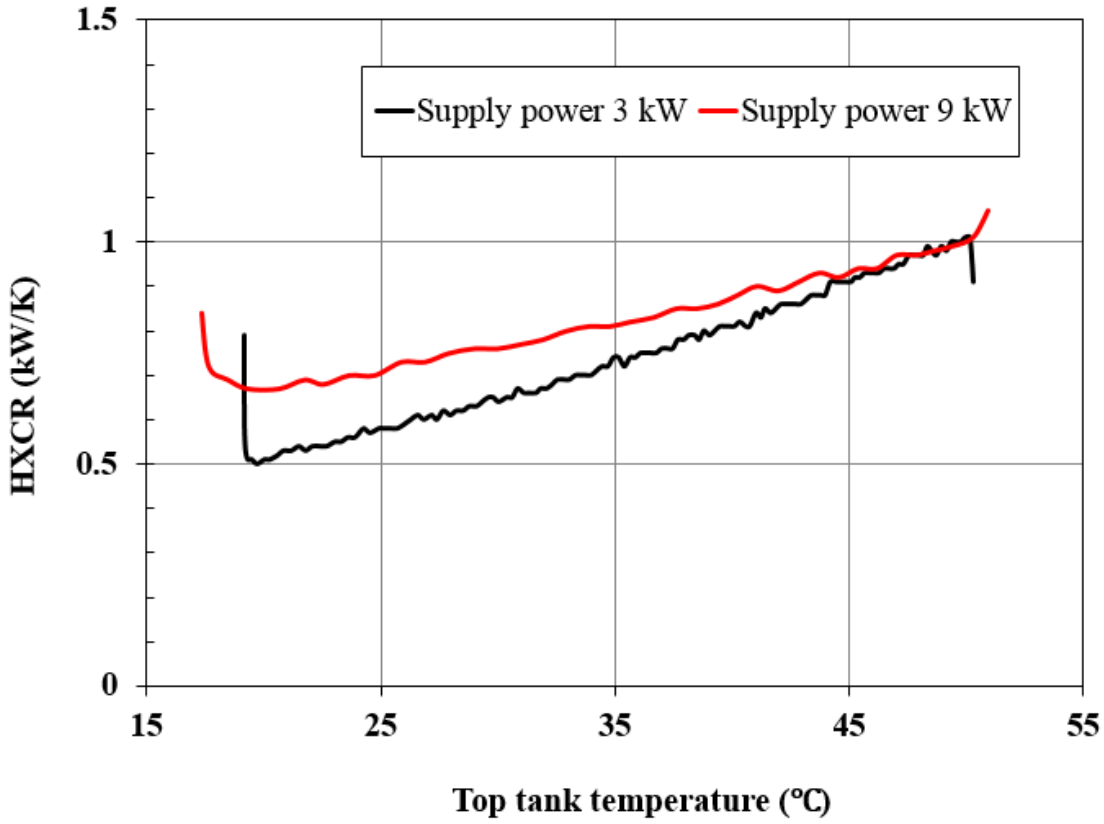

Figure 17 HXCR of the top spiral of the improved tank with a flow rate of 13.8 l/min

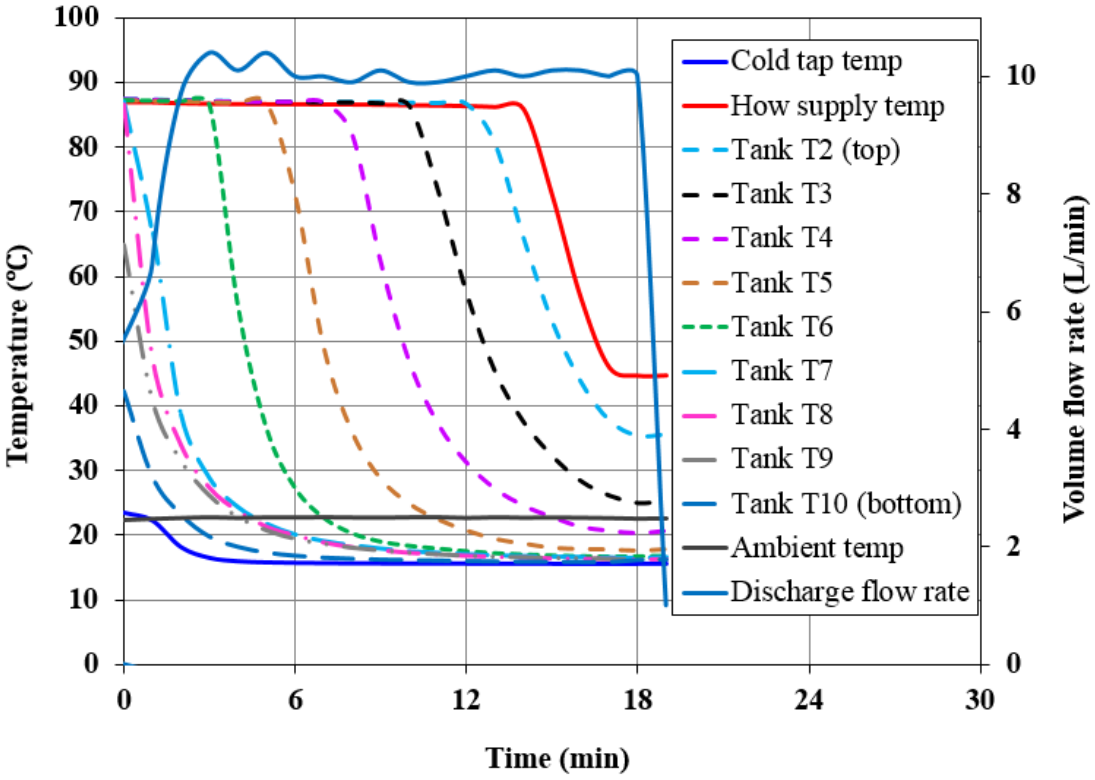

Figure 18 Temperature development of the improved tank during hot water draw-off of 180 l with a flow rate of 10 l/min

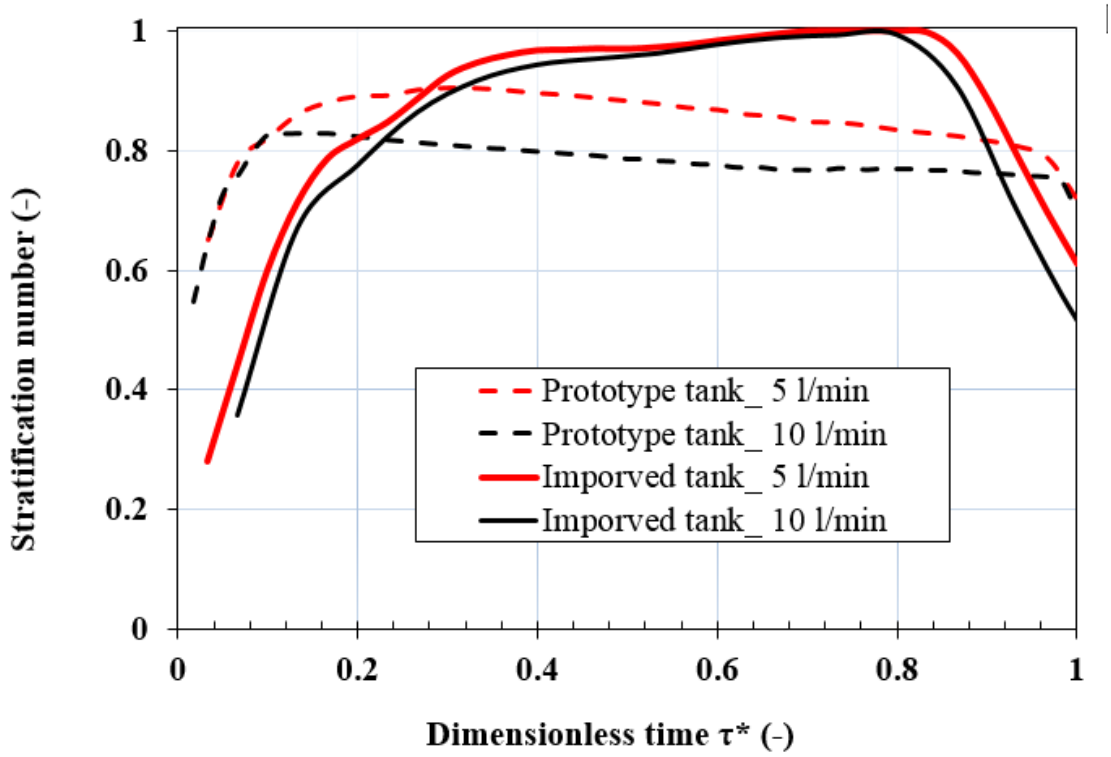

Figure 19 Comparison of the Stratification numbers for the prototype and the improved tanks

Tables:

Table 1. Configurations of the prototype tank and the improved tank

	Prototype tank	Improved tank
Hot supply pipe	Located in the center of the tank	Adopted a pipe connection from the tank top
Length of top spiral	7 m	20.4 m
Length of bottom spiral	28 m	22.5 m

Table 2. Heat content of the PCM under a series of test cycles for the prototype tank

Test cycle No.	Descriptions	Temperature interval	Heat content of PCM	Theoretical heat content of the SAT	Measured /Theoretical
2	Solar charge 6.5 h	23.5 ℃ - 85.9 ℃	3.1 kWh	4.0 kWh	0.78
	Discharge 180 L	85.8 ℃ - 22.9℃	3.2 kWh	4.1 kWh	0.78
8	Solar charge 23.6 h	19.8 ℃ - 86.7 ℃	3.4 kWh	4.1 kWh	0.83
	Discharge 180 L	86.7 ℃ - 18.9℃	3.1 kWh	4.2 kWh	0.74
9	Solar charge 26.5 h	20.3 ℃ - 87.1 ℃	3.6 kWh	4.1 kWh	0.88
	Discharge 270 L	87.1 ℃ - 19.7℃	3.3 kWh	4.1 kWh	0.80
10	Long term charge for 168 h	21.5 ℃ - 82.0 ℃	3.8 kWh	4.0 kWh	0.95
	Long period discharge for 72 h	82.0 ℃ - 9.6℃	3.2 kWh	4.2 kWh	0.76
11	Solar charge 7 h	19.5 ℃ -	3.4 kWh	4.1 kWh	0.83

		86.2 ℃			
	Long standby period (89 h)	86.2 ℃ - 62.8 ℃	1.9 kWh	3.2 kWh	0.60 [1]
12	Long term charge for 96 h	61.7 ℃ - 86.5℃	-	-	-
	Long standby period (240 h)	86.5 ℃ - 41.6 ℃	3.5 kWh	3.7 kWh	0.95
14	Solar charge 48.5 h	34.7 ℃ - 86.4 ℃	3.9 kWh	3.8 kWh	1.03
	Twice discharge of 75 L with 12 h standby period	86.4 ℃ - 41.9 ℃	3.4 kWh	3.7 kWh	0.92
15	Solar charge 6.8 h	28.1 ℃ - 86.2 ℃	3.4 kWh	4.0 kWh	0.85
	Twice discharge of 75 L with 12 h standby period	86.2 ℃ - 42.4 ℃	3.4 kWh	3.7 kWh	0.90
16	Solar charge for 6.5 h	11.6 ℃ - 86.3 ℃	3.8 kWh	4.3 kWh	0.88
	Discharge for 12 h	86.3 ℃ - 12.4 ℃	3.2 kWh	4.3 kWh	0.74

Note: the test cycle number was not continuous because the test cycles aimed to

auxiliary charges were excluded from the assessment.

[1] The ended average tank temperature of Test cycle No. 11 was above the SAT melting temperature (58 ℃) and just sensible heat content was estimated.

Table 3. Heat content of the PCM under a couple of test cycles for the improved version

Test cycle No.	Descriptions	Temperature interval	Heat content of PCM	Theoretical heat content of the SAT	Measured /Theoretical
2	Solar charge 72.3 h with 1.7 L/min	20.2 ℃ - 85.3 ℃	2.4 kWh	4.0 kWh	0.58 [2]
	Discharge 480 L	85.3 ℃ - 22.9℃	3.8 kWh	4.1 kWh	0.91
4	Solar charge 96.2 h with 0.9 L/min	20.9 ℃ - 83.2 ℃	2.9 kWh	4.0 kWh	0.73
	Discharge with a long period of 2 days	83.2 ℃ - 19.7℃	2.4 kWh	4.1 kWh	0.59
7	Solar charge 50.5 h with 12.4 L/min	15.7 ℃ - 87.3 ℃	3.7 kWh	4.2 kWh	0.87
	Discharge 180 L	87.3 ℃ - 21.2℃	2.1 kWh	4.1 kWh	0.51

8	Solar charge 6.2 h with 6 L/min	16.4 ℃ - 84.7 ℃	3.0 kWh	4.1 kWh	0.73
	Discharge 180 L	84.7 ℃ - 19.3 ℃	2.2 kWh	4.2 kWh	0.53
9	Solar charge 48.6 h with 5.7 L/min	18.9 ℃ - 86.8 ℃	3.6 kWh	4.2 kWh	0.87
	Long standby period of more than 7 days	86.8 ℃ -	-	-	- ([3])

[2] It was presumed that supercooling occurred in test cycle No.1.

[3] The heat content during discharge in test cycle No. 9 was indeterminate due to tank thermal stratification from 34 ℃ (bottom) -59 ℃ (top) after 7 days.